ИНСТИТУТ ЯДЕРНОЙ ФИЗИКИ СО АН СССР

A.N. Dubrovin, A.M. Vlasov and A.A. Zholents

INTERACTION REGION of 4×7 GeV ASYMMETRIC B-FACTORY

PREPRINT 89-97

НОВОСИБИРСК

Interaction Region of 4×7 GeV Asymmetric B-Factory*)

A.N. Dubrovin, A.M. Vlasov and A.A. Zholents

Institute of Nuclear Physics
630090, Novosibirsk, USSR

ABSTRACT

This paper deals with the organization of the interaction region of a double ring *B*-factory in the conditions of a comparatively small energy difference between the beams. Besides the well known fact of advantages for the observation of CP violation, this approach gives also the benefit for a storage ring design. The foundations of the approach are given and a variant of the scheme design is presented.

*) Report presented at the *B*-Factory Workshop, Blois, France, June 26—July 2, 1989.

1. INTRODUCTION

In this paper we formulate the solution of the central question of the 4×7 GeV asymmetric *B*-factory design—the question of the interaction region arrangement. Why does it seem very important to us? The matter is that for this beam energy difference (not very small and at the same time not very large) up to day the very possibility of the solution of this problem without luminosity lost compared to the symmetric case was not clear. At the same time the asymmetry of 4×7 GeV is very attractive due to some important reasons. Beginning approximately from this asymmetry all physical advantages of observation the decays of moving *B*-mesons are already realized and one can consider this as a lower limitation on the beam energy difference. On the other hand, one faces with the following dilemma as the asymmetry increase. If the energy difference is not yet very large, it is difficult, if possible at all, to focus both beams at the interaction point (IP). When the energy difference is large, this problem falls away, but another one comes—a high cost of such a mashine.

2. CHOICE OF PARAMETERS

To start up the description of interaction region scheme we would like to base the choice of the dispersion and beta-functions at the IP, emittances and beam energy spreads. We supposed, that

besides a high luminosity our B-factory should certainly possess a monochromatic property, which allows to have an energy resolution in centre-of-mass system about 1 MeV—much less than the beam energy spread. It immediately specifies a strictly determined approach for the choice of parameters—low beam emittances and large dispersion functions at the IP. With an accurate determination of coordinates of the event vertex it gives

$$\sigma_W = \frac{W}{2}\sqrt{\frac{\varepsilon_{h_1}}{J_1} + \frac{\varepsilon_{h_2}}{J_2}}, \qquad (1)$$

where indexes 1, 2 are related to 7 GeV (strong) and to 4 GeV (weak) beam respectively, $W = 2\sqrt{E_1 E_2}$ is the centre-of-mass energy, E is the beam energy, ε_h is the horizontal emittance,

$$J = \frac{\psi^2}{\beta_h}, \qquad (2)$$

ψ is the dispersion function and β_h is the horizontal beta-function at the IP. Our second issue was the size of the storage ring. It seemed to us reasonable to limit circumference of storage rings with 600 m. Therefore, bending radii $R_1 = 60$ m and $R_2 = 30$ m were chosen and having the damping partition numbers of synchrotron oscillations $G_{s_1} = 2$ and $G_{s_2} = 1$ we get for a beam energy spread $\sigma_{\varepsilon_1} = \sigma_{\varepsilon_2} = 0.8 \cdot 10^{-3}$.

To make a better estimation of emittances one needs before a qualitative introduction with beam separation scheme. The beams are separated by a magnetic field due to the difference of the bending radii of strong and weak beams. It is important to us now, that the magnetic field starts just behind the IP (see Fig. 1) and finishes only at the second quadrupole lens. The synchrotron radiation (SR) on this part swings beam emittances and, certainly, does this stronger, when values of the magnetic field and J are higher:

$$\left(\frac{\Delta\varepsilon_h}{\text{cm}\cdot\text{rad}}\right) = 2.5 \cdot 10^{-13} \left(\frac{H}{\text{kGs}}\right)^3 \left(\frac{J}{\text{cm}}\right) \left(\frac{R}{\text{m}}\right) \left(\frac{L}{\text{cm}}\right) \left(\frac{\text{GeV}}{E}\right) \frac{1}{G_h}. \qquad (3)$$

Here $\Delta\varepsilon_h$ is the emittance advance on the separation scheme bends for two interaction regions on the ring, H is the magnetic field, L is the length of the bend, G_h is the damping partition number of the horizontal oscillations. According to (1) and (3) two interaction

regions give for σ_W a minimum value independent on J_1 and J_2. Therefore, one should follow some compromise for a better choice of the magnetic field. For better separation it is preferable to have a higher field, but for smaller swing of emittances the field should be small. We stopped at $H = 4$ kGs and for $L = 2$ m, $J_1 = 60$ cm, $J_2 = 30$ cm we get $\varepsilon_{h_1} = 1.6 \cdot 10^{-6}$ cm·rad, $\varepsilon_{h_2} = 3.6 \cdot 10^{-7}$ cm·rad, and σ_W limit of 1 MeV. Now, the lowering of the bending radius and increase of the damping number for horizontal betatron oscillations for the low energy ring becomes clear. The goal was to make minimum attainable σ_W smaller due to the stronger damping.

The emittance excitation on the storage ring lattice is equal to

$$\left(\frac{\varepsilon_{h_0}}{\text{cm}\cdot\text{rad}}\right) = 2 \cdot 10^{-4} \left(\frac{E}{\text{GeV}}\right)^2 \frac{1}{G_h Q_n^3}. \qquad (4)$$

It is quite reasonable to make $\varepsilon_{h_0} \sim \Delta\varepsilon_h$, that gives $\sigma_W = 1.4$ MeV. To have such emittances one should make $Q_1 = Q_2 = 18$.

Thus, we determined beam energy spreads and horizontal emittances as well as J_1 and J_2 values. Now, we determine beam parameters at the IP and the vertical emittances. A choice of vertical beta-functions is almost evident because it is always beneficial to have them equal to a r.m.s. bunchlength. In our case it is 1 cm for both beams. The choice of β_h and vertical emittances is more problematic. Here one should take several factors into account. The first is the desire to have equal sizes at the IP for both beams. Further, one should provide with realistic emittances, energy spreads and focusing by the first quadrupole lens those beam sizes after the first lens which already allow to use here a special lens influencing oppositely on each beam and finally, beam cross sections at the IP should be matched with beam intensities to provide maximum permissible beam-beam tune shift ξ_v. All these things taking into account we choose $\beta_{h_1} = 40$ *cm*, $\psi_1 = 50$ cm, $\beta_{h_2} = 50$ *cm*, $\psi_2 = 40$ cm and optimal coupling $\varepsilon_{v_1}/\varepsilon_{h_1} = 0.01$ and $\varepsilon_{v_2}/\varepsilon_{h_2} = 0.03$.

Now, for luminosity calculation we need to specify the values of ξ and the collision frequency f. In the separation scheme described below, we suppose to provide separation of the beams already at 2 m from the IP ($f = 75$ MHz). It will allow with $\xi_{v_1} = \xi_{v_2} = 0.05$ and other beam parameters determined above to have a luminosity $L = 5 \cdot 10^{33} \text{cm}^{-2}\text{s}^{-1}$.

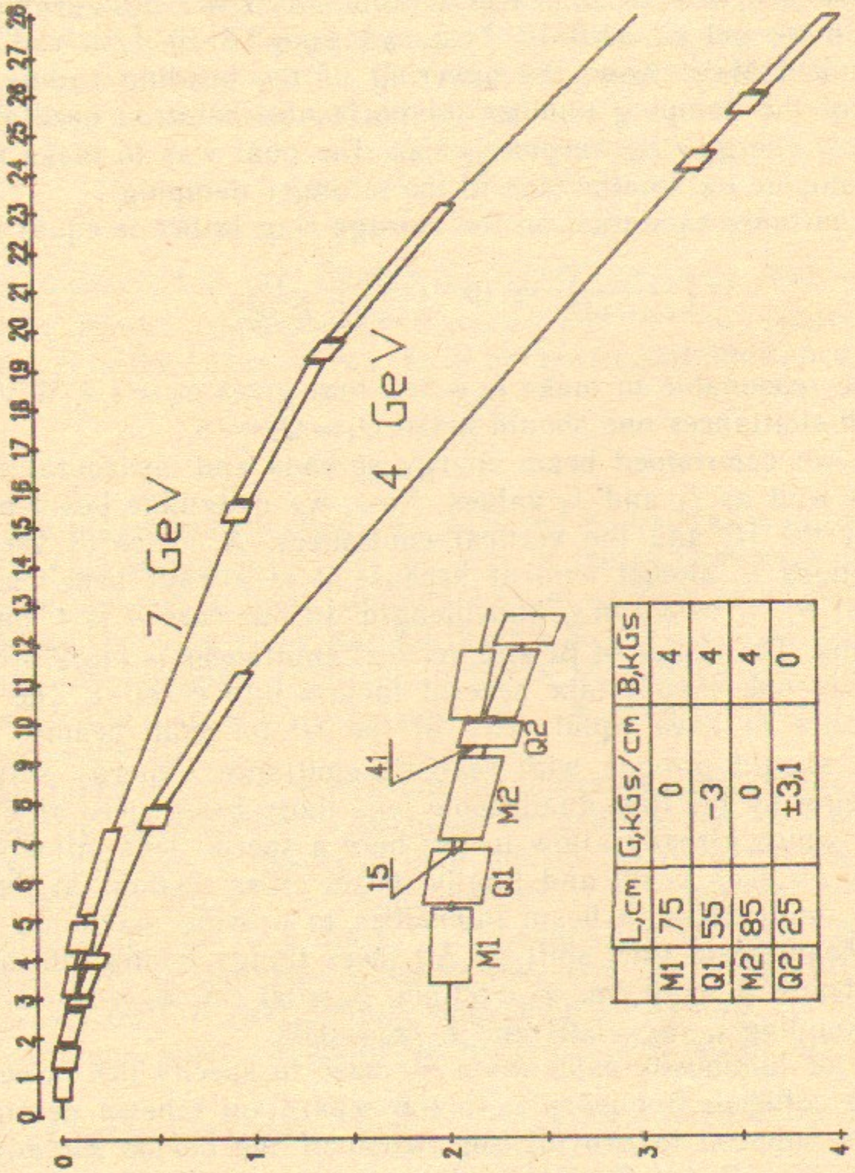

	L,cm	G,kGs/cm	B,kGs
M1	75	0	4
Q1	55	-3	4
M2	85	0	4
Q2	25	±3,1	0

Fig. 1. The interaction region scheme.

3. INTERACTION REGION

3.1. Choice of Separation Scheme

In a magnetic separation scheme with a large energy difference between the beams the separation must be completed before entrance of the nearest to the IP quadrupole lens for the strong beam. In our case of a comparatively small energy difference this lens can be made common for both beams. So the separation scheme begins with initial separation magnet and common vertically focusing quadrupole lens as shown in Fig. 1. The overfocusing effect of the lens on the weak beam and the opposite effect on the strong one are compensated by a double lens with a different gradient sign for each beam in a place where the separation is already sufficient for its installation (see Fig. 2). To increase beam separation, an addi-

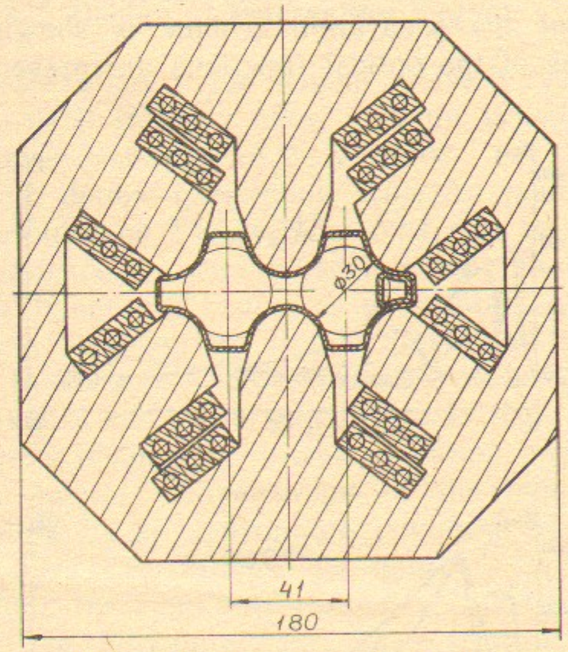

Fig. 2. The double quadrupole lens.

tional dipole magnet is placed between the main and compensating lenses, and the main lens is shifted with respect to weak beam trajectory so that it passes through the same magnetic field as in the magnets. At the same time strong beam is shifted to the lens centre as it moves along the lens, so the magnetic field on its trajectory is gradually reduced. Consequently, the lens separates beams more

effectively than a magnet installed in the same place. A question arises why the separation begins with the magnet rather than with the shifted lens directly. The point is that the main problem of the chosen scheme is the weak beam overfocusing and from that point of view to begin with magnet is preferable. In practice the first lens is moved away from the IP till the value of vertical beta-function holds reasonable.

A position of the double lens is determined as a result of a compromise based on the following considerations. On the one hand, it is desirable to move it away as far as possible for having better beam separation. On the other hand, with a large gap from lens to lens, this lens ceases to compensate the weak beam overfocusing due to decrease of vertical beta-function, and increase of the horizontal beam dimensions in it.

The horizontally focusing lenses can be considered for each beam independently because of already sufficient beam separation.

The layout of the separation scheme is shown in Fig. 1. In Fig. 3 the graphs of the optical functions are presented. We install

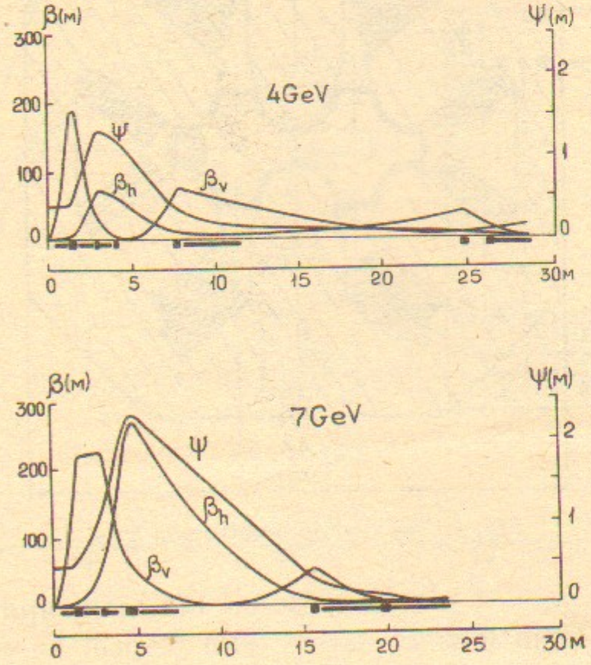

Fig. 3 The behaviour of the optical functions at the interaction region.

the first separation magnet in 40 cm apart from the IP and in the nearest parasitic crossing (2 m apart from the IP) already have the separation of 15 mm. The vertically focusing quadrupole lens is placed in 120 cm apart from the IP and allows to receive at the IP $\beta_v = 1$ cm with the value of β_v-function on the lens about 200 m.

Let us make some explanations of one more feature of scheme — a large value of J at the IP. The choice of comparatively small β_h-functions $\sim$50 cm at the IP leads to rather large values of β_h-functions in the region of horizontally focusing lenses. This fact can be used to excite the required value of J by installing magnets in that place since the advance of betatron tunes from that point to the IP is near the optimal value of $\pi/2$. The rest magnets and lenses shown in Figs 1, 3 provide the appropriate geometry of the rings, β-functions, and zero ψ-function in RF cavities section.

3.2. Design of Interaction Region

A detailed consideration of the scheme element design is beyond the scope of this article. Here we show only the principal possibility of the solution and discuss some of its variants.

Let us start with double quadrupole lens. An example of such a lens design is presented in Fig. 2. This lens can be considered as joining of two quadrupole lenses in such a way that they have a common pole. The hyperbola radius is determined by the requirement of a sufficient aperture for beams and good field quality in the aperture, that in its turn is determined by an air gap at a point of hyperbola cutting. A minimum gap height is fixed by a requirement to let the weak beam synchrotron radiation pass to the common absorber. A partial compensation of the hyperbola cutting influence can be done by an appropriate trimming of a poletip. The list of lens parameters is as follows: the length is 25 cm, the gradient is $\pm$3.1 kGs/cm, the hyperbola radius is 15 mm, a good gradient region along the horizontal axis is $\pm$10 mm. The required dimensions of the useful aperture for the strong beam are $A_x = \pm 9$ mm, $A_z = \pm 18$ mm; for the weak one: $A_x = \pm 9$ mm, $A_z = \pm 5$ mm. The distance between the lens centres is equal to the distance of 41 mm between the beams.

We also consider the variant of the lens with a continuous pole of a neutral sort. In this case, however, we must solve the problem of SR absorption on this pole. On the other hand, the opportunity to

divide the lenses in space appears that probably weakens the requirements for the beam separation.

Another important feature of separation scheme is the placement of a part of its elements inside the detector with a longitudinal magnetic field. To protect these elements from the outer field it was decided to put them in a conically widening iron shield with a compensating superconducting coil around it (see Fig. 4). If the current in the coil per unit length along the axis is the same as in the outer

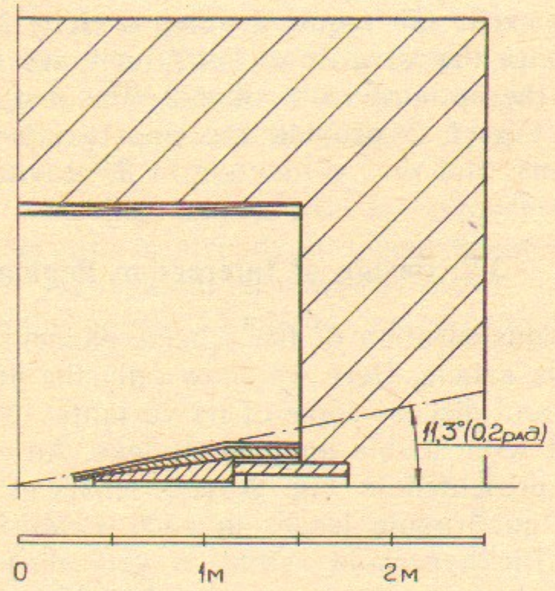

Fig. 4. The detector arrangement.

solenoid then the detector field is not disturbed. However, in this case the field inside the shield is the same as the outer field. It even increases due to a hole in the shield for the magnetic elements, though a part of a longitudinal magnetic flux can pass through their yoke. All that results in increasing of the current in the compensating coil for the reduction of a magnetic flux that saturates the iron shield. Consequently, the homogeneity of the detector field is slightly disturbed (the local inhomogeneity reaches 2—3%).

Among the advantages of such an approach we can mention the opportunity to use iron for dipole magnet and quadrupole placed inside the detector and also rather small solid angle about 2% taken away from a detector.

Let us sketch out the design of the dipole magnet and quadrupole lens (see Figs 5, 6). Both of the elements have superconduc-

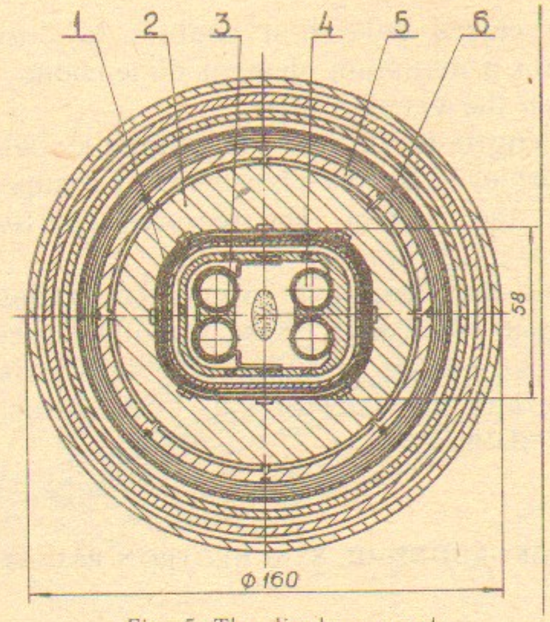

Fig. 5. The dipole magnet:
1 is the dipole superconducting coil; *2* is the dipole iron; *3* is the SR absorber; *4* is nitrogen cooling pipes; *5* is the iron shield; *6* is the superconducting compensating coil.

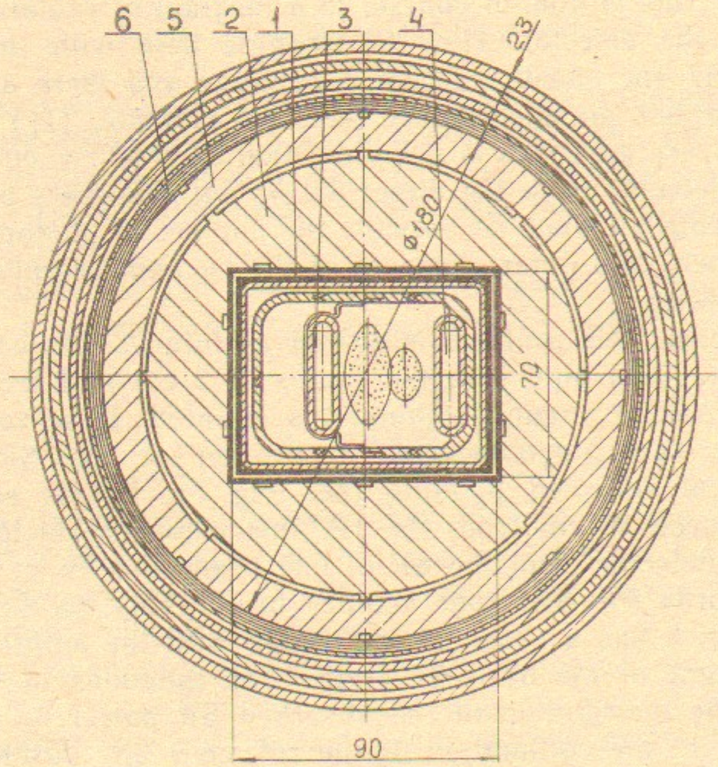

Fig. 6. The quadrupole lens:
1 is the quadrupole superconducting coil; *2* is the quadrupole iron; *3* is the SR absorber; *4* is nitrogen cooling pipes; *5* is the iron shield; *6* is the superconducting compensating coil.

ting coils and a closed yoke that enables to form the necessary magnetic field with a minimum element dimensions. The SR falls on the absorber inside the vacuum pipe.

The magnet length is 75 cm, the magnetic field is 4 kGs. An uniform field is achieved by the placement of a superconducting coil in the air gap of the magnet. The required aperture for beams is $A_x = \pm 7$ mm, $A_z = \pm 13$ mm.

The quadrupole lens length is 55 cm, the gradient is 3 kGs/cm. The lens is designed according to the Panofsky scheme and has an uniform gradient in all the aperture. The lens axis is horizontally shifted with respect to the detector axis by -4 mm at the entrance and by $+12$ mm at the exit.

4. BACKGROUND OF SYNCHROTRON RADIATION

In the interaction region scheme of asymmetric B-factory described above the SR background is a problem of the exceptional importance. This is due, of course, to a location of radiation sources just inside the detector. How to struggle here with the growing back-ground? The question is not a new one and there are a lot of recommendations on this subject (see, for example, [1]). The main feature of every approach is the protection of a thin vacuum pipe of the vertex detector from the direct SR by SR absorbers placed near it and reducing as much as possible the number of photons reflected from absorbers and other elements of the vacuum chamber and hitting the detector.

In our case, this problem is solved as follows. On each side of the vertex vacuum pipe with the radius of 2 cm and the length of 20 cm the special vacuum chamber is situated. It serves simultaneously for two functions—the absorption of the SR and the collimation of reflected photons (see Fig. 7). By its remote end which is placed 26 cm from the IP, this chamber shields vacuum pipe of the detector from the SR of one beam and by its inner surface it absorbs the SR from another beam. This SR falls on the absorber which has a shape of the wedge with the length of 16 cm and the height in the basis of 4 mm. The functions of the wedge consist in the distribution of the absorbed SR power on the larger surface and in the collimation of the reflected SR. Beside this, the reflected SR is collimated by the aperture of the main channel.

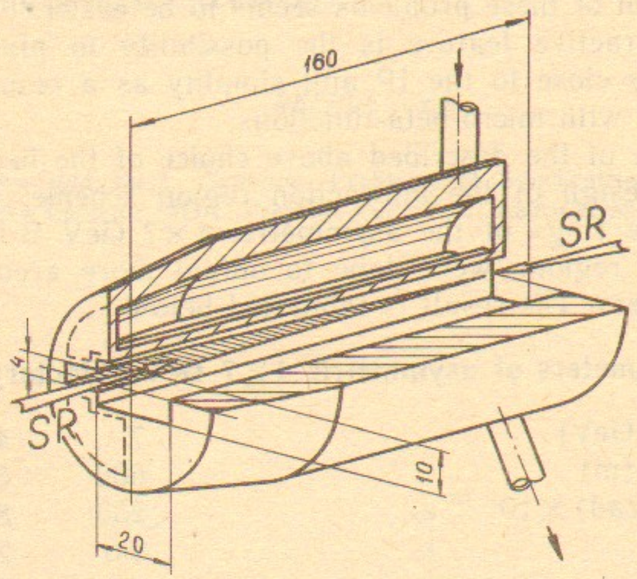

Fig. 7. The collimator and SR absorber.

Thus, photons after one reflection can reach the vacuum pipe of the detector only inside the solid angle of 10^{-2}sr, if the SR falls on the beginning of the wedge and 10^{-4}sr, if the SR falls on the end of the wedge. The improvement can be done by an accurate adjustment of the orbit.

The vacuum chamber described above has to be made from copper and its inner surface should be covered by silver.

5. SUMMARY

Thus, it is in principle clear how to arrange the collisions of 4 GeV and 7 GeV beams. Besides the well known fact of advantages for the observation of CP violation, this approach gives also the benefit for a storage ring design.

The first advantage is the possibility to replace the small number of very intensive bunches by the large number of bunches with a low intensity due to the fast beam separation in the magnetic field. As a result the smaller number of particles per bunch practically takes off the questions of microwave instability and bunch

lengthening. However, all problems of multibunch instability are remained and they become even more complicated. But, nevertheless, the solution of these problems seems to be easier.

Another attractive feature is the possibility to place the first quadrupole lens close to the IP and simplify as a result the problems associated with micro-beta-functions.

On the base of the described above choice of the beam parameters and the design of the interaction region scheme, the calculations of storage rings of the asymmetric 4×7 GeV B-factory with two interaction regions were done to obtain more accurate values for all parameters. The result is tabulated below.

Parameters of asymmetric 4×7 GeV B-factory

Beam energy (GeV)		7	4
Circumference (m)		600	588
Emittance (m·rad) $\times 10^{-10}$	ε_x	250	80
	ε_z	2.5	2.2
		2.5	2.2
Energy spread (10^{-3})		0.9	0.9
Damping partition number	G_s	1.8	1.3
	G_h	1.2	1.7
Bending radius (m)		50	24
Betatron frequency	Q_v	24	25
	Q_h	25	26
Synchrotron frequency Q_s		0.024	0.018
Momentum compaction (10^{-3})		2.8	2.1
Accelerating voltage (MV)		10	4
Bunch length (cm)		1	1
Synchrotron radiation power (MW)		3.2	0.9
Crossing parameters (cm)	β_h	40	50
	ψ	50	40
	β_v	1	1
Particles per bunch (10^{10})		6	8
Number of bunches		150	147
Tune shift	ξ_v	0.05	0.05
	ξ_h	0.008	0.009

Centre-of-mass energy (GeV)	10.6
Centre-of-mass energy spread (MeV), σ_W	1.4
Peak luminosity ($cm^{-2}s^{-1}$) $\times 10^{33}$	5
Number of interaction regions	2

Acknowledgements. The athors are grateful to their colleagues V.A. Lebedev, A.N. Skrinsky, B.M. Smirnov, and P.D. Vobly for interesting and helpful discussions.

REFERENCES

1. *A.P. Onuchin and Yu.A. Tikhonov.* Problems of Synchrotron Radiation Background at the Detector MD-1. Preprint INP 77-77, Novosibirsk 1977.

A.N. Dubrovin, A.M. Vlasov and A.A. Zholents

Interaction Region of 4×7 GeV Asymmetric B-Factory

А.М. Власов, А.Н. Дубровин, А.А. Жоленц

Промежуток встречи 4×7 ГэВ асимметричной В-фабрики

Ответственный за выпуск С.Г.Попов

Работа поступила 23 июня 1989 г.
Подписано в печать 26.06. 1989 г. МН 10296
Формат бумаги 60×90 1/16 Объем 1,3 печ.л., 1,0 уч.-изд.л.
Тираж 290 экз. Бесплатно. Заказ № 97

Набрано в автоматизированной системе на базе фотонаборного автомата ФА1000 и ЭВМ «Электроника» и отпечатано на ротапринте Института ядерной физики СО АН СССР,
Новосибирск, 630090, пр. академика Лаврентьева, 11.